Mass Spectrometry-based Methods for Phosphorylation Site Mapping of Hyperphosphorylated Proteins Applied to Net1, a Regulator of Exit from Mitosis in Yeast*

Susan Loughrey Chen‡, Michael J. Huddleston‡, Wenying Shou§, Raymond J. Deshaies§, Roland S. Annan‡¶, and Steven A. Carr‡‖

Prior to anaphase in *Saccharomyces cerevisiae*, Cdc14 protein phosphatase is sequestered within the nucleolus and inhibited by Net1, a component of the RENT complex in budding yeast. During anaphase the RENT complex disassembles, allowing Cdc14 to migrate to the nucleus and cytoplasm where it catalyzes exit from mitosis. The mechanism of Cdc14 release appears to involve the polo-like kinase Cdc5, which is capable of promoting the dissociation of a recombinant Net1·Cdc14 complex *in vitro* by phosphorylation of Net1. We report here the phosphorylation site mapping of recombinant Net1 (Net1N) and a mutant Net1N allele (Net1N-19m) with 19 serines or threonines mutated to alanine. A variety of chromatographic and mass spectrometric-based strategies were used, including immobilized metal-affinity chromatography, alkaline phosphatase treatment, matrix-assisted laser-desorption post-source decay, and a multidimensional electrospray mass spectrometry-based approach. No one approach was able to identify all phosphopeptides in the tryptic digests of these proteins. Most notably, the presence of a basic residue near the phosphorylated residue significantly hampered the ability of alkaline phosphatase to hydrolyze the phosphate moiety. A major goal of research in proteomics is to identify all proteins and their interactions and post-translational modification states. The failure of any single method to identify all sites in highly phosphorylated Net1N, however, raises significant concerns about how feasible it is to map phosphorylation sites throughout the proteome using existing technologies. ***Molecular & Cellular Proteomics 1: 186–196, 2002.***

Protein phosphorylation is arguably the most important reversible post-translational modification that occurs in cells. Protein kinases and phosphatases add or remove, respectively, phosphate groups that regulate enzymatic activity, protein-protein interactions, and protein tertiary structures. Knowledge of the sites of phosphorylation on a particular protein can aid in understanding the mechanism by which that protein affects a biological pathway.

A variety of techniques are available for detecting phosphorylated peptides. Traditional methods such as TLC and Edman sequencing have the disadvantages that they typically require the use of radioactively labeled sample and either prior knowledge of the protein sequence or the ability to make some assumptions about the peptide sequence. Proteins can be labeled *in vivo* using [^{32}P]orthophosphate or *in vitro* using purified kinase and [γ-^{32}P]ATP. The phosphorylated proteins are enzymatically digested, and the phosphopeptides are isolated by high performance liquid chromatography (HPLC)[1] or two-dimensional TLC and detected by scintillation counting or autoradiography. The HPLC fraction or excised TLC spot is subjected to phosphoamino acid analysis and manual Edman sequencing, monitoring for a loss of radioactivity at each cycle. Because there is typically not an adequate amount of peptide present to detect the non-labeled amino acids, the phosphorylation site must be deduced by comparing the cycle number at which the radioactivity is released with a list of predicted peptides to identify those that contain serine, threonine, or tyrosine at the same position.

Alternative methods for detecting phosphopeptides utilize mass spectrometry (MS) and abrogate the need for radioactivity. MS-based techniques include matrix-assisted laser desorption/ionization (MALDI) to detect peptides that can lose phosphate under conditions of post-source decay (PSD), MALDI analysis of peptides before and after treatment with alkaline phosphatase, and electrospray-based MS methods that detect phosphate-specific marker ions.

From ‡Proteomics and Biological Mass Spectrometry, GlaxoSmithKline, King of Prussia, Pennsylvania 19406 and §Division of Biology, California Institute of Technology, Pasadena, California 91125

Received, December 3, 2001, and in revised form, January 18, 2002

Published, MCP Papers in Press, January 22, 2002, DOI 10.1074/mcp.M100032-MCP200

[1] The abbreviations used are: HPLC, high performance liquid chromatography; BSA, bovine serum albumin; CID, collision-induced dissociation; DTT, dithiothreitol; IMAC, immobilized-metal affinity chromatography; LC-ESMS, liquid chromatography-electrospray ionization mass spectrometry; MALDI, matrix-assisted laser-desorption ionization; MS, mass spectrometry; MS/MS, tandem MS; PSD, post-source decay; TOF, time-of-flight.

Under the appropriate conditions phosphopeptides can undergo collision-induced dissociation (CID) to produce ions that are phosphate-specific (1). CID of serine-, threonine-, and tyrosine-phosphorylated peptides under negative ion conditions results in the formation of phosphopeptide-specific marker ions at *m/z* 79 (PO_3^-) and *m/z* 63 (PO_2^-). Under positive ion conditions serine- and threonine-phosphorylated peptides undergo loss of 98 Da (H_3PO_4) and 80 Da (HPO_3) from the molecular ion, whereas tyrosine-phosphorylated peptides preferentially lose 80 Da. These characteristic fragmentations in the positive and negative ion modes are signatures for phosphopeptides.

Detection of phosphopeptides by MALDI-PSD takes advantage of the phosphorylation-specific losses from the molecular ion (1). MALDI-PSD is performed on reflectron-equipped MALDI-TOF instruments. The molecular ion of interest is selected using an ion gate and undergoes post-source decay in the first field-free region of the instrument. The reflectron then energy-focuses the fragments such that they are detected at the correct mass. Observation of the loss of 80 or 98 Da from the molecular ion is diagnostic for phosphorylated peptides.

Another phosphopeptide detection method for which MALDI-TOF is a convenient readout is the treatment of peptides with alkaline phosphatase (2, 3). This results in an 80-Da shift to lower mass for the previously phosphorylated peptide. Thus, by comparing MALDI spectra recorded before and after alkaline phosphatase treatment, and looking for peaks that disappear from the treated sample, as well as peaks that appear or increase in intensity, it is possible to identify candidate phosphopeptides.

Alkaline phosphatase treatment and PSD are both quick and easy methods for detecting phosphopeptides; however, unfractionated protein digests can be difficult to analyze by these techniques because of their complexity. Furthermore, in cases where the stoichiometry of phosphorylation is very low, the phosphorylated form of the peptide may not be detected in the initial MALDI spectrum. One way to circumvent this problem is to selectively enrich a digest for phosphopeptides using immobilized metal affinity chromatography (IMAC) (4–6). IMAC uses resins that chelate metals such as gallium and iron. When a peptide mixture is passed over an IMAC column negatively charged phosphate groups bind the chelated metal and are retained on the column. Unfortunately, the IMAC interaction is not specific for phosphorylated peptides but is due rather to the acidic nature of the phosphate group. Thus non-phosphorylated peptides containing several acidic amino acids can also bind to the column. Although enriching for phosphopeptides, it is not uncommon for the IMAC eluate to contain a mixture of phosphorylated and non-phosphorylated peptides. To determine which of the peptides in the simplified mixture are phosphorylated, the eluate can be analyzed by MALDI-PSD or alkaline phosphatase treatment.

We have recently reported a multidimensional electrospray MS-based approach to phosphopeptide mapping (7). This technique takes advantage of the formation of phosphospecific marker ions (*m/z* 63 and 79) that occur under CID conditions in the negative ion mode. In the first dimension of the analysis, the tryptic digest of a phosphoprotein is separated by reverse-phase chromatography with a small portion of the eluate being directed to a quadrupole mass spectrometer whereas the remainder of the sample goes to a fraction collector. Marker ions are produced by CID in the source and detected in a selected-ion monitoring mode. An ion chromatogram for *m/z* 63 and 79 is generated and synchronized with the fraction collector to determine which fraction(s) contain phosphopeptides.

Because most fractions will contain a mixture of phosphorylated and non-phosphorylated peptides, with the former often at low stoichiometry, it is usually not sufficient to simply know which fractions contain phosphopeptides. For this reason, a portion of each phosphopeptide-containing fraction is made basic and analyzed in the second dimension by nanoelectrospray MS using precursor ion scanning for *m/z* 79. This experiment specifically detects only the phosphopeptides present in each fraction and reports the *m/z* values that gave rise to the phosphopeptide marker ion. At this point the phosphopeptides in each fraction are sequenced by MS/MS to confirm their identity and determine the exact site(s) of phosphorylation.

To evaluate the capability of our phospho-site mapping strategy, we sought to apply it to the mapping of phosphorylation sites in the mitotic regulatory protein Net1. Net1 is a component of the multifunctional RENT (regulator of the nucleolus and telophase) complex in budding yeast. Prior to exit from mitosis, Net1 sequesters the Cdc14 protein phosphatase subunit of RENT within the nucleolus and inhibits its activity (8–11). During anaphase, Cdc14 is released from Net1 into the nucleus and cytoplasm where it catalyzes exit from mitosis. The mechanism of this release event is not understood but appears to involve the polo-like protein kinase Cdc5.[2] Interestingly, purified Cdc5 promotes the disassembly of recombinant Net1·Cdc14 protein complexes *in vitro* via phosphorylation of Net1. To evaluate the physiological significance of this reaction, we sought to map sites in Net1N that are phosphorylated by Cdc5. Although this approach seemed simple in principle, it proved to be difficult, because Cdc5 phosphorylated many residues in Net1N. Here, we report the multipronged strategy that we employed to comprehensively identify phosphorylation sites even in the very heavily phosphorylated Net1N protein.

[2] W. Shou, R. Azzam, S. L. Chen, M. J. Huddleston, C. Baskerville, H. Charbonneau, R. S. Annan, S. A. Carr, and R. J. Deshaies, manuscript in preparation.

EXPERIMENTAL PROCEDURES

Net1N Expression and Phosphorylation

The Net1N protein, fused to a tag consisting of six histidine residues and a T7 tag (His6-T7-Net1N), was expressed in *Escherichia coli* BL21(DE3) pLysS cells and purified on nickel nitrilotriacetic acid-agarose beads (Qiagen) as described previously for $p28^{Kix1}$ (12). To prepare Net1N phosphorylated by moderate levels of Cdc5 (such that <50% release of Cdc14 from Net1N was obtained), we prepared four tubes, each containing 100 μl of anti-T7 beads (Novagen), 60 μl of His6-T7-Net1N (0.3–0.4 mg/ml), and 100 μl of HEBD (20 mM Hepes, pH 7.2, 150 mM NaCl, 2 mM EDTA, 0.1 mg/ml BSA, 1 mM DTT). The mixture was rotated for 1 h at 4 °C, and beads were washed five times with wash buffer (HBS (20 mM Hepes, pH 7.2, 150 mM NaCl) + 0.2% octylglucoside + 1 mM DTT) and twice with kinase buffer (5 mM Tris·HCl, pH 8.0, 25 mM NaCl, 10 mM $MgCl_2$, 1 mM DTT, 0.1 mg/ml BSA, 1 mM ATP, 10 μg/ml pepstatin + 10 μg/ml chymostatin + 10 μg/ml leupeptin). For the kinase reaction, the beads were supplemented with 100 μl of 2× kinase buffer + 95 μl of H_2O + 2.0 μl of Cdc5 (0.5 mg/ml) and incubated at room temperature for 1 h. The beads were subsequently washed six times with wash buffer and three times with H_2O and eluted three times with 100 μl of 0.1% trifluoroacetic acid. The eluates were pooled and dried under vacuum. Pellets were dissolved in a total of 10 μl of 8 M urea, which was then supplemented with 30 μl of 30 mM Tris·HCl, pH 8.8. 1 μl was loaded on a 10% SDS-polyacrylamide gel and visualized using Coomassie Blue staining.

Evaluation of Net1N Phosphosite Mutants in Cdc14 Release Assay

Cdc5 phosphorylation sites were identified in this sample (see below), and accordingly, His6-T7-Net1N-19m (Ser^{48}, Ser^{56}, Ser^{60}, Thr^{62}, Ser^{64}, Ser^{152}, Ser^{156}, Ser^{178}, Ser^{179}, Ser^{180}, Thr^{192}, Ser^{202}, Ser^{207}, Ser^{242}, Ser^{269}, Ser^{270}, Ser^{280}, Thr^{288}, and Ser^{335} all changed to Ala) was constructed from a T7 promoter-driven His6-T7-Net1N Bluescript plasmid using site-directed mutagenesis (Stratagene).

Different alleles of Net1N were transcribed from the Bluescript T7 promoter and translated in the presence of [^{35}S]methionine using rabbit reticulocyte lysate (TNT quick coupled transcription/translation systems; Promega). For each Net1N mutant, 35 μl of reticulocyte lysate were incubated with 130 μl of HEBD and 60 μl of GST-Cdc14 beads for 1 h at 4 °C. To assemble GST-Cdc14 beads at 4 °C, 60 μl of protein A beads (Sigma) were incubated with 4 μl of anti-GST and 100 μl of HEBD for 1 h, washed four times with HBS + 1 mM DTT, incubated with 15 μl of GST-Cdc14 (0.2 mg/ml) + 150 μl of HEBD for 1 h, and washed six times with HBS + 1 mM DTT. GST-Cdc14 beads that had captured [^{35}S]-labeled Net1N were washed eight times with HBS + 0.2% Triton + 1 mM DTT and twice with kinase buffer, equally distributed into four tubes, and exposed to different amounts of kinase in a 30-μl reaction at 22 °C for 35 min. After the kinase reaction, the supernatant was transferred to new tubes. The beads were washed once with 70 μl of HEBD, and the wash was pooled with the supernatant and precipitated with trichloroacetic acid (10% final) on ice for 30 min. After centrifugation in a microfuge for 10 min, the pellet was saved as "sup." Proteins present on the beads or in the sup were analyzed by autoradiography.

Isolation of Phosphorylated Net1N-19m

His6-T7-Net1N-19m was purified by release from GST-Cdc14 beads upon treatment with Cdc5. 50 μl of GST-Cdc14 beads (1 μg/μl) were incubated with 110 μl of Net1N-19m (0.8 μg/μl) and 110 μl of HEBD for 2 h at 4 °C and washed seven times with wash buffer and once with kinase buffer. Beads from four such tubes were pooled and split into ten tubes of 20-μl beads. Each of these ten tubes was supplemented with 80 μl of 2× kinase buffer, 74 μl of water, and 6 μl Cdc5 and incubated at room temperature for 4 h. Supernatant from every two tubes was pooled, incubated with 100 μl of anti-T7 beads for 2 h at 4 °C, washed seven times with wash buffer and three times with H_2O, and eluted three times with 100 μl of 0.1% trifluoroacetic acid. The eluates were pooled and dried under vacuum. The pellets were dissolved in a total of 7 μl of 8 M urea and later supplemented with 21 μl of 30 mM Tris·HCl, pH 8.8. 0.8 μl of the final product was loaded on a 10% SDS-polyacrylamide gel and visualized by Coomassie Blue dye.

Digestion, Ga^{3+}-IMAC Enrichment, and Mass Spectrometric Analysis of Phosphorylated Net1N Species

Purified recombinant Net1N in 1 M urea, 15 mM Tris·HCl, pH 8.8, and 50 mM ammonium bicarbonate was reduced with 2 mM DTT and alkylated in 20 mM iodoacetamide prior to digestion with trypsin (Promega) at a ratio of 1:20 (w/w). The digest was desalted using a gel loader pipette tip microcolumn (13) packed with POROS R2 (PerSeptive Bioscience). Peptides in the flow-through were captured on a Hypercarb Graphitic Carbon (Hypersil) microcolumn. The microcolumn, packed with 250 μg of Hypercarb was equilibrated and washed with 0.1% formic acid, and peptides were eluted with 2 μl of 60% acetonitrile, 0.1% formic acid.

Ga^{3+}-IMAC Enrichment—Phosphopeptide enrichment of the mixture eluting from the POROS R2 column was accomplished using Ga^{3+}-IMAC, based on the procedure of Posewitz and Tempst (6). The peptide mixture that was eluted from the POROS R2 microcolumn was applied directly to the Ga^{3+}-IMAC microcolumn, which was packed with 2 mg of POROS MC (PerSeptive Biosystems) charged with 80 μl of 100 mM $GaCl_3$ and equilibrated with 0.1% trace metal grade acetic acid. The IMAC column was washed with 30 μl of 0.1% acetic acid, 30 μl of 30% acetonitrile, and 30 μl of 0.1% acetic acid. Peptides were eluted in 15 μl of 200 mM $NaPO_4$, pH 8.4, directly onto a second POROS R2 microcolumn for desalting. The POROS R2 microcolumn was equilibrated and washed with 0.1% formic acid, and peptides were eluted with 2 μl of 60% acetonitrile, 0.1% formic acid.

Alkaline Phosphatase Treatment—Alkaline phosphatase reactions were done directly on the MALDI target. An aliquot of each sample (0.25 μl) was mixed with an equal volume of alkaline phosphatase (calf intestine; Roche Molecular Biochemicals) that had been diluted 1:10 in 100 mM ammonium bicarbonate. The reactions were incubated for 5 min at room temperature followed by addition of 0.5 μl of α-cyano-4-cinnamic acid matrix (10 mg/ml in 50% acetonitrile, 50% ethanol).

LC-ESMS of Intact Net1N—Intact Net1N protein (100 pmol) was acidified with 0.1% trifluoroacetic acid prior to injection on a 0.5 × 150-mm Magic C_{18} column. Protein was eluted with a gradient of 5–60% acetonitrile, and the eluent was split 1:20 before being introduced into the Micromass Q-tof mass spectrometer. The molecular mass of the intact protein was recorded in the positive ion mode. Data were summed and deconvoluted using the Micromass Masslynx with MaxEnt 1 software.

MALDI and MALDI-PSD—Samples for MALDI and MALDI-PSD were mixed 1:1 with α-cyano-4-cinnamic acid matrix (10 mg/ml in 50% acetonitrile, 50% ethanol), and 0.5 μl was spotted on the target. Spectra were acquired in reflectron mode on a Micromass TofSpec SE. Spectra were calibrated externally using two peptide standards. PSD spectra were acquired as single segments. Precursor ions were isolated using a single Bradbury-Neilson ion gate.

MS/MS Sequencing of Phosphopeptides—To sequence the phosphopeptides, approximately one-half of the sample was dried, reconstituted in 2 μl of 50% methanol, 5% formic acid, and transferred to

a nanospray needle (Protana). Nanospray MS/MS mass spectra were collected on a Micromass Q-tof hybrid quadrupole time-of-flight mass spectrometer equipped with a Z-spray source. Data were analyzed using the Masslynx data system.

Digestion and Mass Spectrometric Analysis of Phosphorylated Net1N-19m

Phosphorylation site mapping of the Net1N-19m mutant was done using a multidimensional ESMS-based strategy that has been described previously (7). HPLC was carried out on a Hitachi L6200A system. The flow from the HPLC pumps was split pre-column from 400 μl/min to 4 μl/min using an LC Packings Accurate microflow splitter. Mobile phases were 2% acetonitrile, 0.02% trifluoroacetic acid (Solvent A) and 90% acetonitrile, 0.02% trifluoroacetic acid (Solvent B). Samples were acidified with 0.1% trifluoroacetic acid and then injected onto a 300-μm × 5-mm PepMap C_{18} (LC Packings) cartridge that had been installed in place of the sample loop on the injector (Rheodyne model 8125). The cartridge was washed with 0.1% trifluoroacetic acid, the injector was rotated into the inject position, and the sample was back-eluted off the trap onto a 180-μm × 150-mm PepMap analytical column (LC Packings) using a gradient of 5–50% Solvent B in 20 min and then 50–95% Solvent B in 5 min. The flow was split post-column by a 150-μm microvolume Valco tee inserted into a Micromass nanoflow ion source such that 0.6 μl/min flowed to a 20-μm inner diameter tapered fused silica electrospray tip (New Objectives) and the remainder to a prep line for manual collection of fractions. Electrospray mass spectra were recorded in the negative ion mode on a PE Sciex API-III atmospheric pressure ionization triple quadrupole tandem mass spectrometer equipped with a high pressure collision cell (PE Sciex). Phosphospecific marker ions were generated in the source vacuum prior to the Q1 mass filter by the application of a high orifice voltage.

Fractions that were identified in the phosphospecific LC-ESMS scan to contain phosphopeptides were then analyzed by precursor scan to determine the *m/z* of the phosphopeptides (7). One-fourth to one-half of the fraction was dried, reconstituted in 2 μl of 50% methanol, 10% concentrated ammonium hydroxide, and transferred to a nanoelectrospray needle (Protana). A full scan negative ion spectrum was recorded, followed by a negative ion precursor scan for *m/z* 79 on a PE Sciex API-III triple quadrupole mass spectrometer. Peptides were sequenced using a Micromass Q-tof mass spectrometer equipped with a nanoES source as described above.

RESULTS

Analysis of Net1N Phosphorylation—Net1 accumulates in a hyperphosphorylated form in *cdc14^{ts}* cells arrested in late anaphase at the non-permissive temperature (8). In an earlier study, we found that the Polo-like kinase Cdc5 is necessary to disrupt the RENT complex and to free nucleolar Cdc14 in late mitosis, that elevated Cdc5 activity provokes ectopic mobilization of Cdc14 in pre-anaphase cells, and that the phosphorylation state of Net1 is regulated by Cdc5 during anaphase.[2] These observations prompted us to examine whether Cdc5-mediated phosphorylation could directly destabilize the RENT complex. Indeed, recombinant Cdc5 kinase can disassemble the RENT complex *in vitro* by phosphorylating Net1 and thereby reducing its affinity for Cdc14.[2] In addition, a truncated form of Net1 containing amino acids 1–341 (Net1N) expressed and purified from *E. coli* retains the ability to bind and inhibit Cdc14 (10). We reasoned that if phosphorylation of

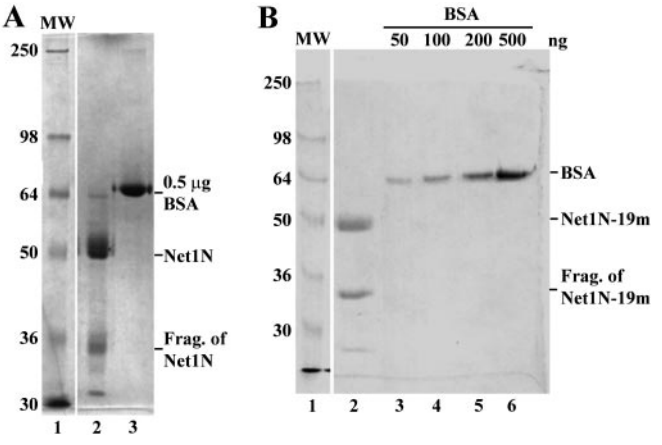

FIG. 1. **Cdc5-phosphorylated His6-T7-Net1N protein samples for mass spectrometry analysis.** Net1N phosphorylated by moderate amounts of Cdc5 (*A*) and Net1N-19m released from GST-Cdc14 beads by Cdc5 (*B*) were loaded, together with molecular weight markers and BSA, on a 10% SDS-polyacrylamide gel and visualized by staining with Coomassie Blue. A fragment (*Frag.*) of Net1N (which reacts to anti-T7 antibodies) was present in both samples.

Net1 by Cdc5 was indeed responsible for disrupting the RENT complex, then a mutant Net1 or Net1N lacking Cdc5 phosphorylation sites should bind Cdc14 even in the presence of active Cdc5. We therefore sought to determine the sites of phosphorylation of Net1N.

Net1N and Net1N-19m proteins were expressed as His6-T7 fusions in *E. coli* and phosphorylated *in vitro* with Cdc5 (Fig. 1). To determine the extent to which Cdc5 phosphorylated Net1N *in vitro*, the molecular masses of the intact protein before and after incubation with purified Cdc5 were determined by LC-ESMS (Fig. 2). The mass of the non-phosphorylated protein was determined to be 40,393 Da, consistent with the average mass calculated for the des-Met1 form of Net1N (40392 Da). After incubation with Cdc5, a heterogeneous distribution of protein molecular masses, each differing by 80 Da, was observed. The range of the mass distribution suggests that each mole of Net1N was modified with 3 to 12 mol of phosphate. However the presence of additional phosphate groups at low stoichiometry could not be ruled out as the spectrum is rather noisy. Mass spectra of multiply phosphorylated proteins are inherently noisy relative to the unphosphorylated protein as the signal is being distributed across multiple forms.

Phosphorylated Net1N was digested with trypsin, and a small aliquot was treated with alkaline phosphatase. MALDI spectra were obtained for the phosphatase-treated and untreated samples and compared. In the treated sample, disappearance of peaks present in the untreated sample and concomitant appearance of new peaks or increases in the intensity of peaks at a mass 80 Da lower represent the cleavage of phosphate from a phosphopeptide to create a non-phosphorylated peptide. Fig. 3 shows that five phosphorylated peptides could be identified in this way from the

unfractionated tryptic digest of Net1N. This number is far fewer than the minimum of 12 suggested by the molecular mass distribution of phosphorylated Net1N.

Because the ionization of phosphopeptides might be suppressed by the presence of large amounts of non-phosphorylated peptides in the unfractionated mixture, we sought to enrich the sample for phosphopeptides using IMAC. The MALDI spectrum of the peptides eluted from the IMAC column is shown in Fig. 4*A*. A number of the peaks in the MALDI spectrum had broad, poorly resolved "satellite peaks" ~90 Da lower in mass. These satellite peaks are formed by metastable decomposition in the field-free region after the ion source. Metastable ions do not possess the full accelerating potential and do not penetrate the ion mirror fully. As a result, they appear at the reflecting detector as broadened peaks of higher apparent mass than expected. In this case, decomposition products resulting from loss of H_3PO_4 appear 90 Da lower in mass from the precursor instead of 98 Da lower. We verified that these were metastable decompositions from phosphopeptides by performing PSD on each apparent precursor and observing the loss of H_3PO_4 at the proper mass in the PSD spectrum (data not shown). In this way we identified 10 phosphopeptides.

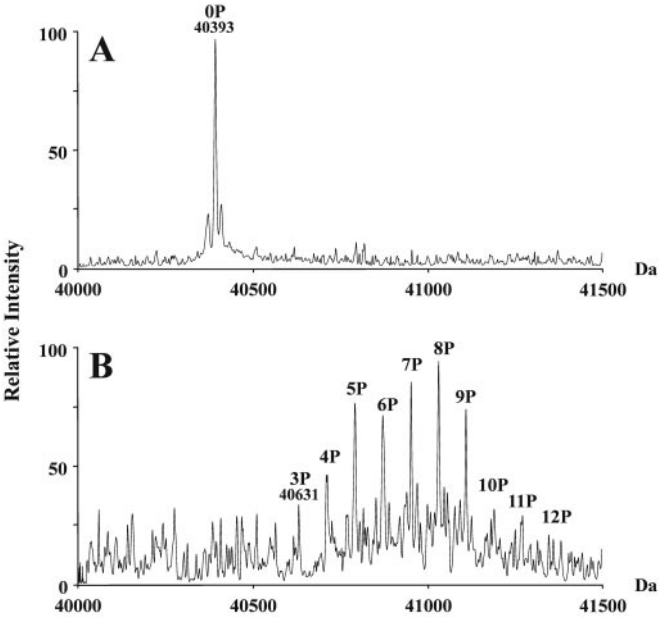

FIG. 2. **Deconvoluted LC-ESMS spectra of Net1N prior (*A*) and subsequent (*B*) to phosphorylation by Cdc5 protein kinase.** 100 pmol of sample were injected onto a 0.5-mm inner diameter PepMap C_{18} reverse-phase HPLC column. The protein was eluted with a gradient of water:acetonitrile:trifluoroacetic acid with 1:20 of the eluate being split to the mass spectrometer and the remaining sample going to a transfer line for fraction collection.

To identify phosphopeptides that did not show an observable metastable product, we treated an aliquot of the IMAC fraction with alkaline phosphatase and compared the MALDI spectra taken before and after treatment (Fig. 4, *A* and *B*, respectively). The spectrum of the treated sample was greatly simplified relative to the untreated sample because of the elimination of the metastable peaks and the collapse of multiply phosphorylated peptides into a single non-phosphorylated peak. Two peptides that had been identified by PSD as being monophosphorylated were at least partially resistant to treatment with alkaline phosphatase (peptides 10 and 14), thus generating a false negative response. Both of these peptides contained a basic residue adjacent to the phosphorylated amino acid. Peptide 10 was also found as the diphosphorylated form (Fig. 4, peptide 11). The second phosphorylation site on this peptide is five residues away from the nearest basic amino acid, suggesting that it should be susceptible to phosphatase treatment. When the sample was treated with alkaline phosphatase the peak for the diphosphorylated peptide disappeared leaving only a monophospho-

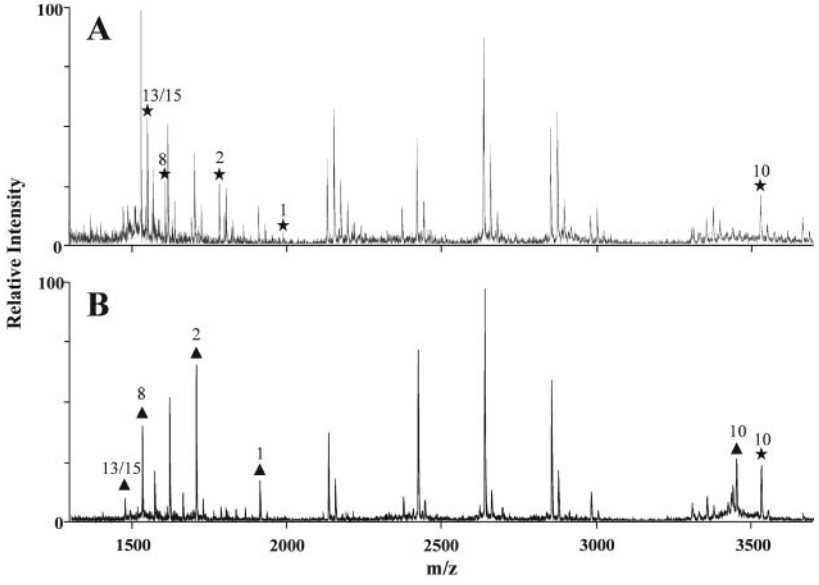

FIG. 3. **MALDI spectrum of the unfractionated Net1N tryptic digest without (*A*) and with (*B*) treatment with alkaline phosphatase.** Peaks marked * indicate those that disappeared upon treatment with alkaline phosphatase with a concurrent appearance of a peak 80 Da lower (▲) in the alkaline phosphatase-treated sample. Only five phosphopeptides were detected in this manner. Peaks are numbered corresponding to the numbering in Table I. Many peaks in the untreated sample were sodium adducts of peptides that disappeared or were reduced in intensity upon treatment with alkaline phosphatase, but these peaks did not have a concurrent appearance of a peak 80 Da lower in mass. Peptide 10 only undergoes partial dephosphorylation (see text for details).

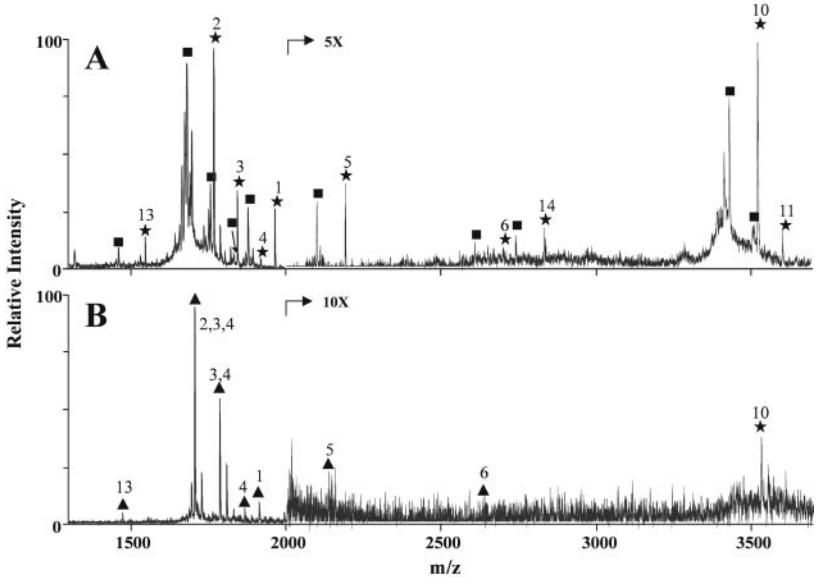

FIG. 4. **MALDI spectrum of Net1N peptides captured by the Ga^{3+}-IMAC column before (*A*) and after (*B*) treatment with alkaline phosphatase.** *A*, peaks that disappear or are greatly diminished after alkaline phosphatase treatment are marked with *stars*. Metastable peaks, denoted by ■, are formed by the loss of HPO_3^{2-} from phosphopeptides in the first field-free region of the flight tube. *B*, The peaks marked ▲ are those that appeared or increased in intensity after alkaline phosphatase treatment. The diphosphorylated peptide 11 is converted to the monophosphorylated peptide 10, which is resistant to treatment to alkaline phosphatase (see text for details). Peaks are numbered corresponding to the numbering in Table I.

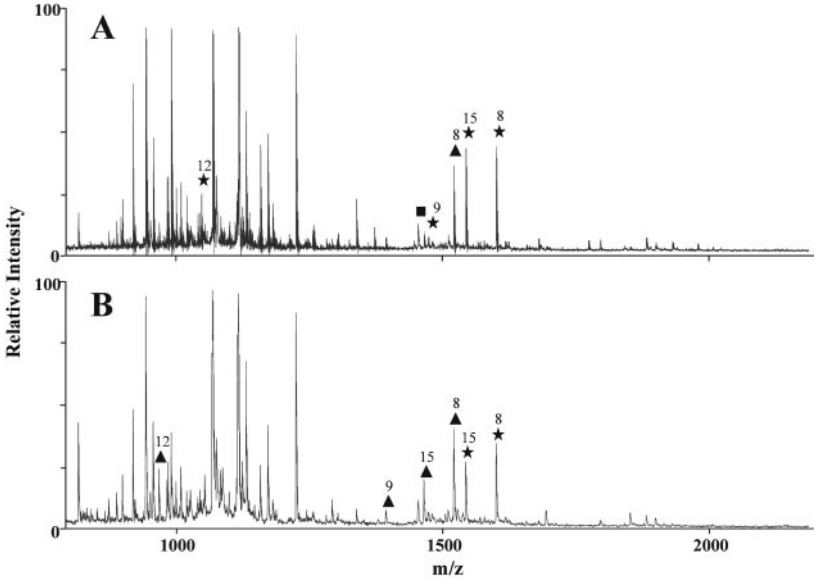

FIG. 5. **MALDI spectrum of peptides eluted from the Hypercarb microcolumn.** The flow-through from the POROS R2 microcolumn was desalted on the Hypercarb microcolumn to determine whether there were peptides that were unable to bind to POROS R2 but would bind to Hypercarb. *A*, spectrum prior to alkaline phosphatase treatment. *Stars* indicate potential phosphopeptide peaks that disappeared or were diminished in intensity after alkaline phosphatase treatment. *B*, spectrum after alkaline phosphatase treatment. ▲ indicates peaks that appear or increase in intensity after alkaline phosphatase treatment. A total of 10 phosphopeptides were detected in this sample, four of which were absent from POROS R2-purified material. Peaks are numbered corresponding to the numbering in Table I.

rylated peptide and no dephosphorylated peptide. In effect, peptide 11 was converted to peptide 10. It is reasonable to suggest that only the site away from the arginine residue is being dephosphorylated. Fig. 3 also suggests that the monophosphorylated peptide 10 is partially resistant to alkaline phosphatase treatment, because it did not become fully dephosphorylated upon treatment with alkaline phosphatase. We have also observed alkaline phosphatase resistance in a synthetic peptide, KRPpSQRHGSKY-NH_2, which contains an arginine close to the phosphoserine (data not shown). In all we identified eight phosphopeptides from the alkaline phosphatase treatment experiment, but no new phosphorylated sequences were discovered.

Experiments in our laboratory with small hydrophilic phosphopeptides have shown that these peptides are not always captured efficiently by POROS R2 (data not shown). Because the IMAC enrichment uses a POROS R2 desalting column before affinity purification, we were concerned about the loss of phosphopeptides from the Net1N tryptic digest. To capture small or hydrophilic phosphopeptides that might flow through the POROS R2 microcolumn, we applied the flow-through to a porous graphitic carbon (Hypercarb) microcolumn. Hypercarb is a material that has been shown to bind some hydrophilic substances better than C_{18}-like resins. Fig. 5 shows the MALDI spectrum of peptides that flowed through the R2 resin, but were captured on Hypercarb, before (Fig. 5*A*) and after (Fig. 5*B*) treatment with alkaline phosphatase. From this we were able to identify four phosphopeptides that were not

TABLE I

Phosphopeptides isolated from Net1N phosphorylated in vitro by Cdc5

Phosphorylated amino acids that were definitively identified are in bold. Residues that could potentially be phosphorylated are in italics.

Peptide	Sequence	Amino acids	M_r
1	TNMAQSAGDA**pS**LQYANLR	38–55	1989.9
2	SANV**pS**FTPS*Y*FNQSR	56–70	1783.8
3	*S*ANV**pS**FTP*S*YFNQSR + 2P	56–70	1863.8
4	**pS**ANV**pS**FTP**pS**YFNQSR	56–70	1943.8
5	VILKNEIDLDDSAPV**pS**LYK	137–155	2211.1
6	SKLNNGSPQ*S*VQPQQQI*P**SSS***GVLR + 1P	160–184	2715.4
7	LNNGSPQ*S*VQPQQQIP*SSS*GVLR + 1P	162–184	2500.2
8	KRPP**pT**GTTTTTTIR	188–201	1609.9
9	RPP*TG**TTTTTT***IR + 1P	189–201	1481.8
10	IVSNNSDDEDEDIGER**pS**FLPPPTQPQSPPIR	226–256	3528.6
11	IVSNN**pS**DDEDEDIGER**pS**FLPPPTQPQSPPIR	226–256	3608.6
12	IS**pS**GIDAGKK	257–266	1054.5
13	IK**pS**SIVEEDIVSR	267–279	1553.8
14	SSIVEEDIVSR**pS**ATVDPDK**pT**KQQR	269–292	2847.4
15	SATVDPDK**pT**KQQR	280–292	1552.8

present in the R2/IMAC fraction.

The overall coverage of tryptic peptides from the Net1N sequence was analyzed by peptide mass mapping, comparing peaks in the MALDI spectrum of the unfractionated tryptic digest to the theoretical tryptic map of Net1N. To fill in several sequence gaps in the MALDI data, we analyzed an additional aliquot of the Net1N tryptic digest by positive ion LC-ESMS and searched the data for the masses of missing peptides (± phosphate; data not shown). In this way we identified two additional potential phosphopeptides as members of an 80-Da difference pair. We were able to partially sequence one of these peptides (LNNGSPQSVQPQQIPSSSGVLR + 1P; amino acids 162–184; molecular mass 2500.2 Da) by MS/MS, though the site of phosphorylation was not definitively assigned. We were unable to sequence the remaining peptide, but its mass matched that of the sequence LQVVLVPPSLQATMPIGFGYGPTIAESSQLLPNR + 1P (amino acids 4–37; molecular mass 3744.0 Da). The overall sequence coverage based on the combined MALDI and LC-ESMS data was 98%.

Putative phosphopeptides identified by the presence of a metastable peak, by alkaline-phosphatase treatment, by PSD (data not shown), or from the positive ion LC-ESMS data were sequenced by MS/MS to confirm the identity of the phosphopeptide and determine the site(s) of phosphorylation. In total, we sequenced 15 of 16 possible phosphopeptides (Table I). For those 15 phosphopeptides, 12 specific sites of phosphorylation were determined. In only three cases (peptides 160–184, 162–184, and 189–201) were we unable to specify the exact location of the phosphate group. In these three cases, the fragmentation data were not sufficient to determine whether there was one specific site of phosphorylation or a mixed population of singly phosphorylated peptides, modified at different sites.

Analysis of Net1N Mutants—Based on the mapped sites (Table I), as well as other potential sites, a series of Ser/Thr → Ala mutants were constructed (Table II). If Cdc5 phosphorylation on any of these sites was critical in disrupting the binding of Cdc14 to Net1, then the non-phosphorylatable Net1 mutants should form a complex with Cdc14 that is resistant to disruption by Cdc5. To test this hypothesis, radiolabeled mutant and wild-type Net1N proteins bound to GST-Cdc14 beads were treated with increasing amounts of Plx1, a Polo-like kinase from *Xenopus* that is closely related to Cdc5. Because Plx1 (Polo-like kinase in *Xenopus*; see Ref. 14) can disrupt the RENT complex *in vitro* (data not shown) and is expressed at high levels in insect cells, we used Plx1 instead of Cdc5 in these tests. We verified independently that Net1N phenotypes were equivalent in assays using Plx1 or Cdc5 (data not shown). The amount of Net1N released into the supernatant or that remained bound to GST-Cdc14 beads was analyzed using autoradiography.

As an example, 0.3 μl of Plx1 released ~90% of wild-type Net1N from GST-Cdc14 beads, whereas 1 μl of Plx1 had to be used to release ~80% of Net1N (Ser^{48} Ser^{60} Ser^{64} Ser^{242} Ser^{335} → Ala) (Fig. 6*A*). Thus, this mutant allele of Net1N was ~3-fold more resistant to Plx1 than wild-type Net1N. A list of mutants and their phenotypes are listed in the *top portion* of Table II.

Despite the large number of phosphorylated sites that had been mutated, Net1N-19m could still be phosphorylated by Cdc5 and was still capable of dissociating from Cdc14 in the *in vitro* assay when the level of Plx1/Cdc5 was elevated 3-fold (data not shown). One possibility was that one or more critical Cdc5 phosphorylation sites were overlooked using the combined MALDI-IMAC mapping strategy or that Cdc5 phosphorylated secondary sites on Net1N once the primary sites were eliminated. To address these possibilities, Net1N-19m protein released from GST-Cdc14 beads by Cdc5 was subjected to phosphorylation site mapping for the following two reasons: 1) Net1N-19m contains many fewer phosphorylation sites

TABLE II
Net1N mutants and their phenotypes

Mutant	Net1N mutant alleles[a]	-Fold defect
1	S60 S64 S242 S335	<3
2	S60 S64 S242 S48	3
3	S60 S64 S242 S335 S48 (5m)	3
4	S60 S64 S242 S335 S48 S269 S270	3
5	S60 S64 S242 S335 S48 S269 S270 S207	3
6	S60 S64 S242 S335 S48 S269 S270 S207 S152 S56	3
7	S60 S64 S242 S335 S48 S152 S156 S280	3
8	S60 S64 S242 S335 S48 S269 S270 S207 S152 S56 S156 S280	3
9	S60 S64 S242 S335 S48 S269 S270 S207 S152 S56 S156 S280 S202 T62 S178 S179 S180	3
10	S60 S64 S242 S335 S48 S269 S270 S207 S152 S56 S156 S280 S202 T62 S178 S179 S180 T192 T288 (19m)	3
11	S60 S64 S242 S335 S48 S269 S270 S207 S152 S56 S156 S280 S202 T62 S178 S179 S180 T192 T288 S12 T16 T26 S30 S31	10
12	S60 S64 S242 S335 S48 S12 T16 T26 S30 S31	10
13	S60 S64 S242 S48 S12 T16 T26 S30 S31	10
14	S60 S64 S242 S335 S48 T26	<3
15	S60 S64 S242 S335 S48 T26 S30 S31	10–30
16	S60 S64 S242 S335 S48 T26 S30 S31 T38 T282	10
17	S60 S64 S242 S335 S48 T26 S30 S31 S223 S224 S301 T302	10
18	S60 S64 S242 S335 S48 S269 S270 S207 S152 S56 S156 S280 S202 T62 S178 S179 S180 T192 T288 T16 T26 S30 S31 S223 S224 S228 S231 S301 T302	10[b]
19	S60 S64 S242 S335 S48 S30 S31 (7m)	30
20	S60 S64 S242 S335 S48 S30 S31 T16 S223 S224 S228 S231 S295 S301 T302 T194 T195 T196 T197	30

[a] All indicated amino acids were mutated to alanine.
[b] High background level of release when kinase was not included in the reaction, suggesting weakened interaction between the mutant Net1N and Cdc14.

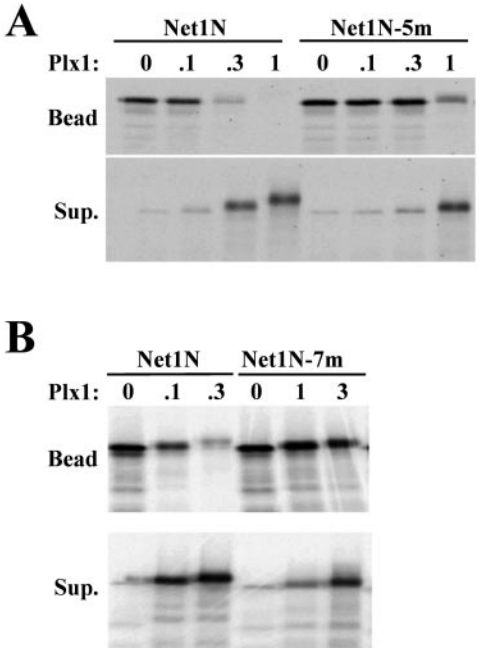

FIG. 6. **Mutant alleles of Net1N show a range of defects in the *in vitro* release assay.** [^{35}S]-Labeled wild-type or mutant Net1N was captured by GST-Cdc14 beads and treated with the indicated amounts of Plx1. Net1N protein released into the supernatant (*Sup.*) or that remained bead-bound (*Bead*) was analyzed by autoradiography.

than Net1N, which simplifies the task of mapping; and 2) key phosphorylation site(s) on Net1N-19m that influence the interaction between Net1 and Cdc14 should be phosphorylated in all released protein molecules.

To improve our confidence in the phosphopeptide mapping results we used an ESMS-based multidimensional mapping strategy developed in our laboratory over the past few years and proven to be highly reliable for all phosphorylation mapping problems. The phosphopeptide-specific LC-ESMS ion trace for a tryptic digest of Net1N-19m phosphorylated by Cdc5 shows a highly complex profile (Fig. 7*A*), indicating that despite the large number of mutations Net1N-19m was still extensively phosphorylated by Cdc5. All of the HPLC fractions shown to contain phosphopeptides by means of the phosphopeptide-specific trace were analyzed by precursor scans for *m/z* 79, to identify the phosphopeptides present in each fraction. The precursor ion scan for one such fraction is shown in Fig. 7*C*. This spectrum shows more than 20 peaks corresponding to various charge states for two unique peptide sequences phosphorylated to different extents. Comparison of the precursor scan of this fraction (Fig. 7*C*) with the positive ion spectrum for the same fraction (Fig. 7*B*) shows that precursor-ion scanning for *m/z* 79 can detect phosphopeptides that are not readily observed in the full-scan mass spectra. The latter contain many non-phosphorylated peptides, some of which obscure the signals for the phosphorylated peptides. For example the highly phosphorylated 332–371 peptide would have gone undetected if not for the selectivity of the precursor ion scan. To confirm the sequence assignments and determine the exact site(s) of phosphorylation for phosphopeptides identified in the precursor ion scans,

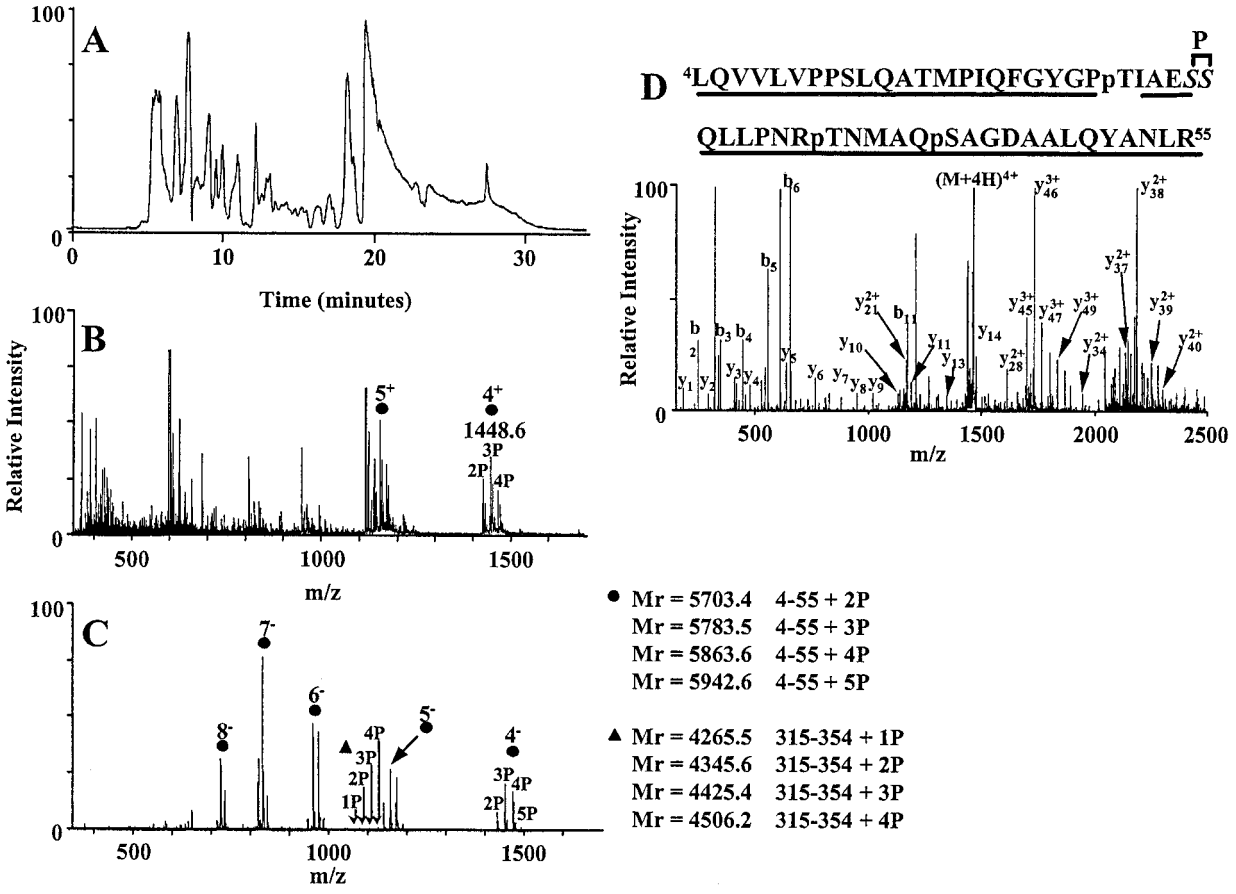

FIG. 7. *A*, selected ion chromatogram of the reverse-phase LC separation of the tryptic digest of Net1N-19m. The digest (130 pmol) was injected on a 180-μm $\times$ 15-cm PepMap C_{18} column flowing at 4 μl/min. The flow was split such that 0.6 μl of the sample went to the mass spectrometer and the remainder to a prep line for manual fraction collection. The mass spectrometer was set to detect *m/z* 63 and 79, diagnostic markers for phosphate loss. The chromatogram represents the sum of the signals for these two markers. *B*, positive ion spectrum acquired. *C*, precursor scan of one fraction from the reverse-phase LC separation of the Net1N-19m tryptic digest. One-fourth to one-half of the fraction was dried and reconstituted in 2 μl of 50% methanol, 5% concentrated ammonium hydroxide. First a negative ion spectrum was acquired and then the precursor scan for ions producing *m/z* 79 marker ions. Another portion of the fraction is dried down and brought up in 50% MeOH, 5% formic acid. *D*, a quadruply phosphorylated, 4+ ion with *m/z* 1466 from this fraction was selected for tandem mass spectrometry.

each phosphopeptide was analyzed by MS/MS. The MS/MS spectrum of the 4+ charge state for the quadruply phosphorylated 4–55 peptide identified in the precursor ion scan of fraction 6 (Fig. 7*C*) is shown in Fig. 7*D*. Because of the size of the peptide (5863 Da), the spectrum is quite complex. Nevertheless, the high quality of the data, which has resolution sufficient to determine the charge states for each fragment ion, allowed us to assign three of the phosphate groups unequivocally, whereas the fourth could be narrowed down to one of two adjacent serines. Altogether, we were able to sequence 16 of the 20 phosphopeptides identified from the precursor ion scans. These sequences, along with the proposed sequences for the other phosphopeptides, are listed in Table III.

Of the 16 phosphopeptides that were sequenced from the mutant Net1N-19m, only six specific phosphorylation sites could be identified definitively. On the other hand, an additional 20 sites were shown to be potentially phosphorylated. This is in stark contrast to the phosphopeptides sequenced from the wild-type Net1N, for which 12 sites were definitively assigned in 15 phosphopeptides. The apparent heterogeneity in the mutant suggests that many of these sites were nonspecifically phosphorylated by Cdc5 in the absence of the preferred phosphorylation sites.

More Net1N mutants were constructed based on the new mapping data, and their propensities to release Cdc14 in a Cdc5-dependent manner are summarized in the *lower half* of Table II. One of the most severe mutants (Ser^{60} Ser^{64} Ser^{242} Ser^{335} Ser^{48} Ser^{30} Ser^{31} $\rightarrow$ A) displayed a 30-fold defect in the release assay (the effect of 3 μl of Plx1 on Net1N-7m is similar to that of 0.1 μl of Plx1 on wild-type Net1N; see Fig. 6*B*).

CONCLUSIONS

In its unphosphorylated state, a recombinant, truncated form of Net1 (Net1N) from *Saccharomyces cerevisiae* binds to

TABLE III

Phosphopeptides isolated from Net1N-19m phosphorylated in vitro by Cdc5

Phosphorylated amino acids that were definitively identified are in bold. Residues that could potentially be phosphorylated are in italics.

Sequence	Amino acids	M_r
LQVVLVPP*S*LQA*T*MPIQFGYGP*T*IAE*SS*QLLPNR*T*NMAQ*S*AGDAALQYANLR + 2P	4–55	5699.9
LQVVLVPP*S*LQA*T*MPIQFGYGP*T*IAE*SS*QLLPNR*T*NMAQ*S*AGDAALQYANLR + 3P	4–55	5779.9
LQVVLVPPSLQATMPIQFGYGP**pT**IAE*SS*QLLPNR**pT**NMAQ**pS**AGDAALQYANLR + 4P	4–55	5859.9
LQVVLVPP*S*LQA*T*MPIQFGYGP*T*IAE*SS*QLLPNR*T*NMAQ*S*AGDAALQYANLR + 5P	4–55	5939.9
KRPPAG*TTT*TTTIR + 1P	188–201	1579.8
KRPPAG*TTT*TTTIR + 2P	188–201	1659.8
V*ST*PLAR + 1P	210–216	822.4
QIYPPP*SS*K + 1P	217–225	1095.5
QIYPPP*SS*KIV*S*NN*S*DDEDEDIGER + 1P	217–241	2883.3
QIYPPP*SS*KIV*S*NN*S*DDEDEDIGER + 2P	217–241	2963.3
IVSNN**pS**DDEDEDIGER	226–241	1885.8
AAIVEEDIV**pS**R	269–279	1280.6
AA**pT**VDPDKAK	280–289	1094.5
LL*SG**T*PIM*ST*M*T*PNR + 1P	293–307	1697.8
LL*S*G*T*PIM*ST*M*T*PNR + 2P	293–307	1777.8
V*TL**T*GQR + 1P	308–314	853.4
VVSEHAHKNELVFSASASSSAFANGGTGGSIDVEHHHHHH + 1P	315–354	4262.9
VVSEHAHKNELVFSASASSSAFANGGTGGSIDVEHHHHHH + 2P	315–354	4342.9
VVSEHAHKNELVFSASASSSAFANGGTGGSIDVEHHHHHH + 3P	315–354	4422.9
VVSEHAHKNELVFSASASSSAFANGGTGGSIDVEHHHHHH + 4P	315–354	4502.9

immobilized recombinant Cdc14. Phosphorylation of Net1N by the Cdc5 protein kinase results in the release of Net1N from Cdc14. Cdc5 incorporates from 3–12 phosphates per molecule of Net1N. What molecular mass analysis of the intact phosphoprotein does not reveal, however, is whether all Net1N molecules phosphorylated on a given number of sites, *e.g.* 8, are all phosphorylated on the same octet of residues. Thus, substantially more than 12 different residues on Net1N may be phosphorylated by Cdc5. The sites of phosphorylation on Net1N were mapped using a variety of biochemical and mass spectrometric techniques, including alkaline phosphatase treatment and immobilized metal affinity chromatography, which revealed at least 12 phosphorylation sites on 15 phosphopeptides. Based on these sites of phosphorylation and other criteria, a mutant was created in which 19 serines or threonines were modified to alanine to test whether precluding phosphorylation of these sites by Cdc5 could prevent release of Net1N from Cdc14. Despite the large number of mutations created, the Net1N-19m mutant was still phosphorylated by Cdc5, and this phosphorylation resulted in the dissociation of Net1N-19m from Cdc14.

To determine what Cdc5 phosphorylation sites persisted in Net1N-19m, a phosphate-specific marker ion mass spectrometric strategy was used. A total of 20 phosphopeptides were sequenced, but only six phosphorylation sites were definitively assigned, with another 20 sites flagged as being potentially phosphorylated. Importantly, a mutant of Net1N that lacks a subset of sites identified in the first and second round of phosphorylation site mapping shows a profound inability to release tightly bound Cdc14 upon treatment with Cdc5 protein kinase. Remarkably, however, this mutant does not exhibit any detectable defect in the release of Cdc14 from Net1 during the exit from mitosis in budding yeast. These results establish two important points. First, even though it is technically feasible to identify those sites that mediate the phosphorylation-dependent release of Cdc14, identification of the relevant sites required a multipronged strategy. MALDI-based mapping of Net1N, even when coupled to different upstream chromatographic separations (reverse-phase, Hypercarb, IMAC) was unable to identify all of the sites whose phosphorylation by Cdc5 precludes association with Cdc14. This result has significant implications for proteomic strategies to map phosphorylation sites in regulatory proteins on a global scale. It is evident from our data that any strategy that is based on a single chromatographic separation technique or that employs only one form of ionization is unlikely to uncover all of the phosphorylation sites in heavily phosphorylated proteins. Given that some of the regulatory proteins that have been characterized in most detail are phosphorylated either on multiple sites (*e.g.* Rb, Cdc25) or by multiple distinct protein kinases (*e.g.* p53), the data that emerge from simplistic schemes to map phosphorylation sites throughout the proteome are likely to miss many of the critical phosphorylations that regulate cellular biology. Rather, it appears that dedicated analyses of individual proteins are likely to produce the most reliable picture of the phosphorylation status of a protein until major advances in technology enable determination of phosphorylation sites in low abundance proteins on a global scale.

A second significant conclusion that emerges from the work described here and in Shou *et al.*[2] concerns the importance of making mutations in *cis* to confirm hypotheses about how a

particular phosphorylation event(s) regulates a biological process. The evidence supporting the hypothesis that phosphorylation of Net1 by Cdc5 triggers release of Cdc14 is quite strong. 1) Cdc14 is not released from Net1 in Cdc5 mutants, 2) Cdc14 is precociously released from Net1 in cells that overproduce Cdc5, 3) Cdc5 controls the phosphorylation state of Net1 *in vivo*, and 4) Cdc5 can disassemble RENT complexes *in vitro* and is able to interfere directly with Cdc14-Net1 interaction via phosphorylation of Net1.[2] Nevertheless, a mutant of Net1 that no longer releases Cdc14 upon treatment with Cdc5 *in vitro* exhibits no defect in release of Cdc14 during progression through anaphase *in vivo*. Thus, although Cdc5 is involved in the release of Cdc14 from Net1, our data suggest that its involvement is indirect. Many studies have implied a link between a biological response and phosphorylation of a specific protein based on correlative data or based on data generated with overproduced proteins. Our observations underscore the importance of mapping phosphorylation sites and making cis mutations to confirm the existence of specific regulatory circuits.

* The costs of publication of this article were defrayed in part by the payment of page charges. This article must therefore be hereby marked "*advertisement*" in accordance with 18 U.S.C. Section 1734 solely to indicate this fact.

¶ To whom correspondence may be addressed: GlaxoSmithKline, 709 Swedeland Rd. UW 2940, King of Prussia, PA 19406. Tel.: 610-270-6532; Fax: 610-270-6608; E-mail: roland_s_annan@gsk.com.

‖ To whom correspondence may be addressed: Millennium Pharmaceuticals, 640 Memorial Dr., Cambridge, MA 02139. Tel.: 617-679-7090; Fax: 617-679-7071; E-mail: carr@mpi.com.

REFERENCES

1. Annan, R. S., and Carr, S. A. (1996) Phosphopeptide analysis by matrix-assisted laser desorption time-of-flight mass spectrometry. *Anal. Chem.* **68,** 3413–3421
2. Liao, P. C., Leykam, J., Andrews, P. C., Gage, D. A., and Allison, J. (1994) An approach to locate phosphorylation sites in a phosphoprotein: mass mapping by combining specific enzymatic degradation with matrix-assisted laser desorption/ionization mass spectrometry. *Anal. Biochem.* **219,** 9–20
3. Zhang, X., Herring, C. J., Romano, P. R., Szczepanowska, J., Brzeska, H., Hinnebusch, A. G. and Qin, J. (1998) Identification of phosphorylation sites in proteins separated by polyacrylamide gel electrophoresis. *Anal. Chem.* **70,** 2050–2059
4. Andersson, L., and Porath, J. (1986) Isolation of phosphoproteins by immobilized metal (Fe^{3+}) affinity chromatography. *Anal. Biochem.* **154,** 250–254
5. Muszynska, G., Andersson, L., and Porath, J. (1986) Selective adsorption of phosphoproteins on gel-immobilized ferric chelate. *Biochemistry* **25,** 6850–6853
6. Posewitz, M. C., and Tempst, P. (1999) Immobilized gallium(III) affinity chromatography of phosphopeptides. *Anal. Chem.* **71,** 2883–2892
7. Annan, R. S., Huddleston, M. J., Verma, R., Deshaies, R. J., and Carr, S. A. (2001) A multidimensional electrospray MS-based approach to phosphopeptide mapping. *Anal. Chem.* **73,** 393–404
8. Shou, W., Seol, J. H., Shevchenko, A., Baskerville, C., Moazed, D., Chen, Z. W. S., Jang, J., Shevchenko, A., Charbonneau, H., and Deshaies, R. J. (1999) Exit from mitosis is triggered by Tem1-dependent release of the protein phosphatase Cdc14 from nucleolar RENT complex. *Cell* **97,** 233–244
9. Straight, A. F., Shou, W., Dowd, G. J., Turck, C. W., Deshaies, R. J., Johnson, A. D., and Moazed, D. (1999) Net1, a Sir2-associated nucleolar protein required for rDNA silencing and nucleolar integrity. *Cell* **97,** 245–256
10. Traverso, E. E., Baskerville, C., Liu, Y., Shou, W., James, P., Deshaies, R. J., and Charbonneau, H. (2001) Characterization of the Net1 cell cycle-Dependent regulator of the Cdc14 phosphatase from budding yeast. *J. Biol. Chem.* **276,** 21924–21931
11. Visintin, R., Hwang, E. S., and Amon, A. (1999) Cfi1 prevents premature exit from mitosis by anchoring Cdc14 phosphatase in the nucleolus. *Nature* **398,** 818–823
12. Shou, W., and Dunphy, W. G. (1996) Cell cycle control by *Xenopus* p28Kix1, a developmentally regulated inhibitor of cyclin-dependent kinases. *Mol. Biol. Cell* **7,** 457–469
13. Erdjument-Bromage, H., Lui, M., Lacomis, L., Grewal, A., Annan, R. S., McNulty, D. E., Carr, S. A., and Tempst, P. (1998) Examination of micro-tip reversed-phase liquid chromatographic extraction of peptide pools for mass spectrometric analysis. *J. Chromatogr. A* **826,** 167–181
14. Kumagai, A., and Dunphy, W. G. (1996) Purification and molecular cloning of Plx1, a Cdc25-regulatory kinase from Xenopus egg extracts. *Science* **273,** 1377–1380